Notes

Atom Transfer Radical Polymerization of a Semifluorinated Triblock Copolymer of Poly(methyl methacrylate)-*b*-Polypentafluorostyrene-*b*-Poly(methyl methacrylate)

Yoon Soo Ko, Ju Hyun Oh, Kyu Bo Kim, Han Sun Park, Min Sung Kim, and Yong Ku Kwon*

*Department of Polymer Science and Engineering, Inha University, Incheon 402-751, Korea*

Introduction

Controlled radical polymerization (CRP) technique has attracted recent scientific and industrial attention in the field of polymer chemistry.[1-3] It can be achieved by rapid propagation and reversible termination or transfer reaction that are much faster than the irreversible termination reaction which enables polymer chains to grow more slowly and continuously with conversion. There are largely three systems in CRP such as nitroxide mediated polymerization (NMP),[4-6] atom transfer radical polymerization (ATRP),[6-10] and reversible addition fragmentation chain transfer (RAFT).[11-13] Especially in ATRP, a radical can be formed reversibly polymeric materials by transfer of a halogen from an alkyl halide to a transition metal complex. The reversible formation of active radicals from dormant alkyl halides determines the concentration of radicals and the deactivation process to form the alkyl halides was usually dominant in ATRP to maintain the low radical concentration.[14] Therefore, in ATRP, molecular weights, polydispersity, compositions and architecture can be easily controlled with conversion.

Block copolymers have received much scientific and technological attention due to their ability to self-assemble into a series of periodic ordered micro-structures *via* microphase separation between the constituent block segments.[15] There are a number of applications by using their phase-separated morphology both in the solid state and in solutions.[16,17] To synthesize these block copolymers with predetermined molecular weights and low polydispersity, anionic polymer-

*Corresponding Author. E-mail: ykkwon@inha.ac.kr

ization is usually employed.[18] However, its use is highly limited due to the strict reaction conditions such as extremely low temperature, exclusion of moisture and impurity, and stringent drying. Recently, ATRP has been used in such a manner to build block copolymers of radically polymerizable monomers. In this process, active halogens are incorporated at the chain ends of polymers to form macroinitiators. In addition, the ATRP process produces an end-functional polymer that can be used as a macroinitiator for further polymerization with additional monomers, resulting in a multicomponent block copolymer.[19-22] In the present study, we synthesized a well-defined, semi-fluorinated triblock copolymer of poly(methyl methacrylate)-*b*-polypentafluorostyrene-*b*-poly(methyl methacrylate) (PMMA-*b*-PPFS-*b*-PMMA) by ATRP technique. It has been known that fluorinated chains are less miscible than the corresponding hydrogenated chains due to their extremely low surface energy, and the large size of fluorine atoms of the pentafluorostyrene units of PMMA-*b*-PPFS-*b*-PMMA prevents the rotation around the polymer backbones, possibly making the molecules rigid.[23] By analogy with low molar mass compounds, we expect that the suitable composition of the pentafluorostyrene units of PMMA-*b*-PPFS-*b*-PMMA easily produces a self-assembled, ordered morphology through the microphase separation between component block segments. The nonpolar nature of pentafluorostyrene units based on the weak intermolecular forces due to a symmetric distribution of most C-F bonds of the pentafluorostyrene units of PMMA-*b*-PPFS-*b*-PMMA may lead to a well-defined thin film morphology through different wettability of component building blocks on the substrate, which will be also discussed in the present study.

Results and Discussion

A novel semifluorinated, symmetric triblock copolymer containing the semifluorinated PPFS midblock and PMMA endblocks was successfully synthesized by ATRP of the
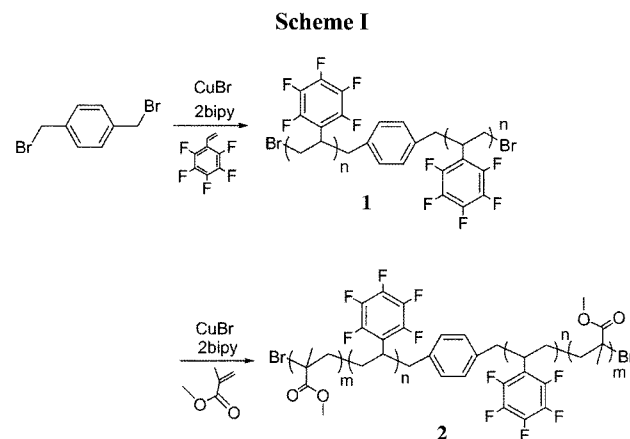
Scheme I

dibromo-ended PFS macroinitiator. Scheme I describes the synthetic procedure of Br-PPFS-Br macroinitiator (**1**) and PMMA-*b*-PPFS-*b*-PMMA (**2**).

The macroinitiator **1** was synthesized by ATRP using a CuBr/2,2'-dipyridyl system and the relative mole ratio of monomer/initiator/CuBr/ligand was 200/1/1/4, and the reaction was carried out at 110 °C for 48 h. The molecular weight and polydispersity of **1**, measured by GPC, were given as 20,400 (53% conversion) and 1.27. The ATRP of **2** was carried out at 60 °C using a CuBr/2,2'-dipyridyl system and the relative mole ratio of monomer/initiator/CuBr/ligand was 800/1/1/4. The molecular weight and polydispersity of **2** were measured as 42,000 (28% conversion) and 1.31. The polydispersity for **2** was slightly larger than that of **1**, which was mainly due to the short period of polymerization time, 2 h. However, the further increase in the reaction time resulted in the continuous increase in molecular weight of **2**, which also caused the rapid increase of the solution viscosity to make stirring in the reaction solution become rather difficult. We measured DSC heating and cooling scan data for both **1** and **2** with a scanning rate of 10 °C/min. For **1**, a single glass transition, along with the endothermic hysteresis peak, was observed at near 103 °C, whereas we observed two transitions at 105 °C and 123 °C for **2** which were attributed to the glass transitions of PPFS and PMMA block segments, respectively. The measurements were carried out at least three times in each experiment to achieve statistically significant averages. The T_g of the PPFS block segments of **2** was slightly higher than one measured from **1** because of the PMMA block segments, connected to the PPFS block segments in a block sequence. These data also confirm the successful synthesis of **2** by ATRP.

An overview of the typical small angle X-ray scattering data of as-cast samples of **2**, measured during heating from room temperature to 200 °C is shown in Figure 1. Specimens for the SAXS measurement had dimensions of 6(length) ×2(width)×1(thickness) mm³, obtained by cutting the films, obtained by solution-casting from chloroform. For SAXS measurements, these samples were placed between two heating blocks and supported by thin films of Kapton™ films to prevent a loss of samples at high temperatures. Data were collected at every 10 °C during heating from 50 °C with a heating rate of about 1 °C/min and the samples were annealed for 10 min at each temperature prior to the data collection. The temperature was controlled with an accuracy of ± 1 °C in the temperature range 30~200 °C. For good counting statistics, scans were made at 5 min at each temperature.

Curve (a) shows the SAXS data obtained at 120 °C. A shallow maximum in intensity is seen at a Q of about 0.34 nm⁻¹ with a corresponding dimension of approximately 18.5 nm. The weakness and broadness of the peak, characteristic of disordered block copolymers, clearly indicates that the copolymer is in the disordered state. A weak intensity maxi-
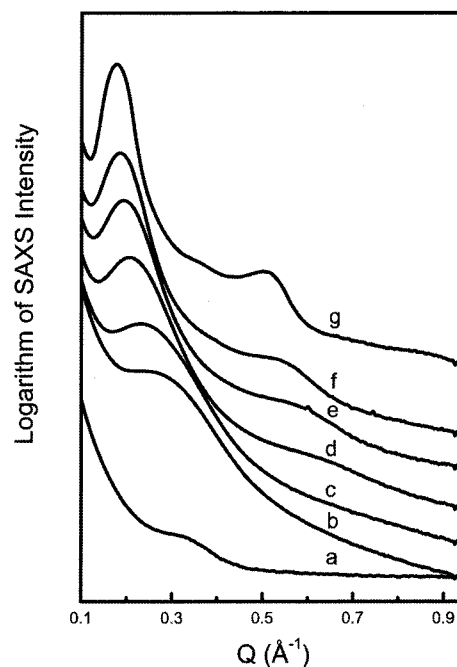

Figure 1. Temperature dependence of the small angle X-ray scattering profiles of PMMA-*b*-PPFS-*b*-PMMA as a function of the scattering wavevector Q. Measurements were made at (a) 120 °C, (b) 130 °C, (c) 140 °C, (d) 150 °C, (e) 160 °C, (f) 170 °C and (g) 180 °C.

mum was thought to be appeared due to correlation hole effect[24,25] which is a signature of the disordered state. Curves (b) through (g) measured in the temperature range of $130 \leq T$ (°C) ≤ 180 illustrate the increasing intensities of the major diffraction peaks. One may interpret that the existence of a few scattering peaks in this temperature range is caused by the correlation hole effect. However, this possibility may be excluded because the intensities of the major scattering peak seen in curves (b) through (g) increase with temperature and shift towards a lower Q, which clearly indicates that it appears due to the microphase separation between the PPFS and PMMA dissimilar blocks at high temperatures.

The fast growth of the peak intensity reflects a rapid progress of the microphase separation between dissimilar PPFS and PMMA blocks upon heating, initiated from the disordered state of the film specimen of PMMA-*b*-PPFS-*b*-PMMA. The shift in the peak position indicates the lamellar thickening with increasing the structural perfection of the domain structure, driven by continuous development of microphase separation between component blocks. The absence of the high order scattering peaks was partly due to the fast progress of the microphase separation of the PPFS and PMMA blocks initiated from the disordered state, resulting in a structural imperfection of the heterogeneous domain structure. The observed X-ray peaks at 180 °C appear at relative positions 1:2:3, which corresponds to a lamellar phase with long period of 37 nm ($d=2\pi/Q^*$), estimated based
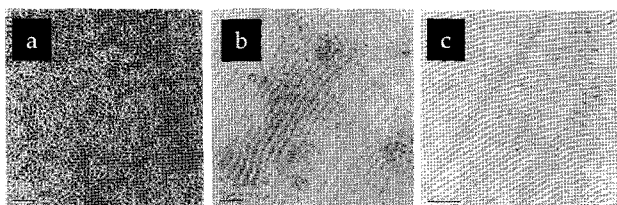
Figure 2. TEM images of PMMA-*b*-PPFS-*b*-PMMA annealed at (a) 130 °C, (b) 160 °C and (c) 180 °C.

on the position of the first-order SAXS peak at Q^*=0.18 nm^{-1}. As could be expected from the molecular weight data under the assumption of similar densities for the PMMA and PPFS blocks, the volume fraction of the constituting PPFS and PMMA blocks of **2** should be similar to display a lamellar morphology.

Figures 2(a), (b) and (c) show the TEM images of **2**, annealed at 130, 160 and 180 °C during 24 h under vacuum, respectively. The film specimens of **2** were obtained by solution-casting from THF. The solvent was evaporated slowly at room temperature for about 24 h and the cast films were then annealed in a vacuum for additional 24 h. The annealed samples were then located within the epoxy resins, curable at room temperature, and microtomed at room temperature. It has been known that the variation in individual chemistry of each block leads to a change in block incompatibility which eventually affects the microphase separation behavior of block copolymers. In Figure 2(a), we found a disordered morphology, whereas a highly ordered, lamellar morphology was observed in Figures 2(b) and (c). The constituent PMMA and PPFS block segments tend to segregate each other to have a periodic ordered microstructure *via* microphase separation. The long period of the lamellar phase of **2** measured in Figure 2(b) was approximately 35 nm.

Supporting Information Available: Experimental procedure for the syntheses of **1**, **2**, their ^{1}H NMR, DSC data. The material is available on the Internet at http://www.polymer.or.kr.

References

(1) K. Matyjaszewski, Ed., *Advances in Controlled/Living Radical Polymerization*, ACS Symposium Series 854, Washington DC, 2003.

(2) K. Matyjaszewski and J. Xia, In *Handbook of Radical Polymerization*, K. Matyjaszewski and T. Davis, Eds., John Wiley & Sons, Inc., Hoboken 2002.

(3) K. Matyjaszewski and J. Xia, *Chem. Rev.*, **101**, 2921 (2001).

(4) R. Jean and B. Rebecca, *J. Polym. Sci. Part A: Polym. Chem.*, **45**, 2015 (2007).

(5) C. Konn, F. Morel, E. Beyou, P. Chaumont, and E. Bourgeat-Lami, *Macromolecules*, **40**, 7464 (2007).

(6) S. Abraham, J. H. Choi, J. K. Lee, C. S. Ha, and I. Kim, *Macromol. Res.*, **15**, 324 (2007).

(7) K. Matyjaszewski, *J. Macromol. Sci. Pure. Appl. Chem.*, **34**, 1785 (1997).

(8) M. Kamigaito, T. Ando, and M. Sawamoto, *Chem. Rev.*, **101**, 3689 (2001).

(9) N. V. Tsarevsky and K. Matyjaszewski, *Chem. Rev.*, **107**, 2270 (2007).

(10) Y. J. Kwark, J. Kim, and B. M. Novak, *Macromol. Res.*, **15**, 31 (2007).

(11) E. Rizzardo, J. Chiefari, B. Y. K. Chong, F. Ercole, J. Krstina, T. P. T. Le, R. T. A. Mayadunne, G. F. Meijs, C. L. Moad, G. Moad, and S. H. Thang, *Macromol. Symp.*, **143**, 291 (1999).

(12) G. Moad, R. T. A. Mayadunne, R. Ezio, M. Skidmore, and S. H. Thang, *Macromol. Symp.*, **192**, 1 (2003).

(13) J. M. Lee, O. H. Kim, S. E. Shim, B. H. Lee, and S. Choe, *Macromol. Res.*, **13**, 236 (2005).

(14) H. Fischer, *J. Polym. Sci. Part A: Polym. Chem.*, **37**, 1885 (1999).

(15) I. W. Hamley, *The Physics of Block Copolymers*, Oxford University Press, New York, 1998.

(16) D. Hu, Z. Cheng, G. Wang, and X. Zhu, *Polymer*, **45**, 6525 (2004).

(17) Y. Cai, M. Hartenstein, and A. H. E. Mueller, *Macromolecules*, **37**, 7484 (2004).

(18) N. Hadjichristidis, M. Pitsikalis, S. Pispas, and H. Iatrou, *Chem. Rev.*, **101**, 3747 (2002).

(19) R. Paris, J. L. D. L. Fuente, and J. Luis, *Eur. Polym. J.*, **44**, 1403 (2008).

(20) K. Dayananda, B. S. Pi, B. S. Kim, T. G. Park, and D. S. Lee, *Polymer*, **48**, 758 (2007).

(21) E. Amado, C. Augsten, K. Maeder, A. Blume, and J. Kressler, *Macromolecules*, **39**, 9486 (2006).

(22) W. R. Dichtel, K. Y. Baek, J. M. J. Frechet, I. B. Rietveld, and S. A. Vinogradov, *J. Polym. Sci. Part A: Polym. Chem.*, **44**, 4939 (2006).

(23) C. W. Bunn and E. R. Howells, *Nature*, **174**, 549 (1954).

(24) K. Mori, K. Hasegawa, and T. Hashimoto, *Polym. J.*, **17**, 799 (1985).

(25) T. Hashimoto, Y. Ijichi, and L. J. Fetters, *J. Chem. Phys.*, **89**, 2463 (1988).